Kinetic, Mechanistic, and Modeling Study of the OH-Radical-Initiated Oxidation of Di-*n*-butoxymethane (DNBM)

T. Maurer, H. Geiger, I. Barnes,* and K. H. Becker

FB 9-Physikalische Chemie, Bergische Universität GH Wuppertal, Gaussstrasse 20, D-42097 Wuppertal, Germany

L. P. Thüner[†]

Centro de Estudios Ambientales del Mediterraneo, Parque Tecnológico, Calle Charles R. Darwin 14, 46980 Paterna, Valencia, Spain

Received: May 23, 2000; In Final Form: September 14, 2000

FTIR product studies of the OH-radical-initiated oxidation of di-*n*-butoxymethane (DNBM) in the presence of NO_x were performed in an indoor photoreactor and in the outdoor simulation chamber EUPHORE in Valencia, Spain. The reaction products observed in both reaction chambers were *n*-butoxymethyl formate (NBMF), propionaldeyhde, and di-*n*-butyl carbonate (DNBC). In the indoor reactor yields for NBMF and propionaldeyhde of 77 ± 15 and 78 ± 16 mol % were obtained in the system DNBM/MeONO/NO_x/air/$h\nu$ and 88 ± 18 and 69 ± 14 mol % in the system DNBM/H_2O_2/NO_x/air/$h\nu$, respectively. In the outdoor chamber, yields of 80 ± 8 and 44 ± 11 mol % were obtained after sunlight irradiation of a DNBM/NO_x/HONO/air mixture. For di-*n*-butyl carbonate (DNBC), an upper limit of ≤10 mol % was estimated for both reaction chambers. In the indoor photoreactor small amounts of *n*-butyl formate (NBF) and *n*-butoxymethyl butyrate (NBMB) were also detected with upper limits of 3 mol % for each compound. Bimolecular rate coefficients for the reactions of NBMF and DNBC with OH radicals were determined in the indoor photoreactor using the relative rate technique. Values of $k_{OH+NBMF} = (8.00 \pm 0.91) \times 10^{-12}$ cm^3 s^{-1} and $k_{OH+DNBC} = (7.07 \pm 1.64) \times 10^{-12}$ cm^3 s^{-1} were obtained. NBMF was synthesized and authentic samples were used for calibration. A photochemical mechanism was developed to describe the OH-initiated degradation of di-*n*-butoxymethane (DNBM) in the presence of NO_x. The reaction scheme was tested by comparison of computer box model calculations and experimental data. Experimentally obtained and modeled concentration−time profiles for selected reactants are in excellent agreement.

1. Introduction

Ethers are an important class of automotive fuel additives.[1] These compounds enhance the octane level, increase the efficiency of combustion, and reduce the emission of atmospheric pollutants, e.g., hydrocarbons, CO, and particles.[2−5] The possible industrial application of a large number of new oxygenated compounds such as acetals or esters is currently under discussion.[6] For example, both classes of compound are being considered as alternative solvents.

The compound under investigation here, di-*n*-butoxymethane (DNBM), is currently under consideration as a potential diesel fuel component to improve the atmospheric properties of the fuel exhaust. It has been shown that the addition of formaldehyde acetals with the general structure $ROCH_2OR$ to diesel fuel significantly reduces the emission of particulate matter from diesel engines,[5] with DNBM being particularly effective in this respect.

However, the widespread use of these organic compounds will result in their release to the atmosphere in significant quantities and thus the potential arises for possible adverse effects on tropospheric chemistry. It is well-known, for example, that the reformulation of fuel by oxygenated VOCs (volatile organic compounds) increases the exhaust concentration of aldehydes[7] and the discovery of methyl *tert*-butyl ether (MTBE) in groundwater and reservoirs used for drinking water[8] has resulted in the prohibition of MTBE as a fuel additive in California from the beginning of the year 2003.[9] These examples show the necessity to improve the knowledge about the kinetic, mechanistic, and environmental behavior of oxygenated VOCs and their reaction products in the troposphere prior to their widespread application.

In continuation of previous work on the OH radical kinetics of a series of acetals,[10] the present study is focused on the product formation in the OH-initiated oxidation of di-*n*-butoxymethane (DNBM) in the presence of NO_x and also the further reactions of the products. Time-resolved product concentrations were obtained from experiments in both an indoor photoreactor and an outdoor simulation chamber.

Mechanistic studies on tropospheric VOC oxidation are often limited to the detection of the primary reaction products. Reaction mechanisms, which are derived from these experimental data, have not usually been subject to validation by comparison of the measured product concentrations against model calculations. In other instances, where no suitable experimental results are available, reaction mechanisms are

* To whom correspondence should be addressed. E-mail: barnes@physchem.uni-wuppertal.de. Phone: +49-202-439-2510. Fax: +49-202-439-2505.

[†] Present address: Bergische Universität GH Wuppertal.

10.1021/jp001901x CCC: $19.00
Published on Web 11/04/2000

postulated without any further verification. Both methods result in the transfer of considerable uncertainty to the results of models when applied, e.g., to the modeling of field data. As a consequence, this work also includes the development of an explicit photochemical degradation mechanism, which was constructed using the results obtained from the photoreactor experiments. The reaction scheme was developed by comparison of simulated and experimental concentration−time profiles.

Altogether, the present work provides a detailed kinetic, product, and modeling study on the OH-initiated oxidation of di-*n*-butoxymethane in the presence of NO_x.

2. Experimental and Chemical Modeling System

The different experimental systems used for the present investigations are described only briefly here. Details can be found in the literature.[11,12]

2.1. Indoor Photoreactor. The majority of the experiments were carried out in a 1080 L quartz-glass indoor photoreactor equipped with a built-in White mirror system. OH radicals were generated either by the UV photolysis of hydrogen peroxide (H_2O_2) using 32 low-pressure mercury lamps (Philips TUV 40, $\lambda_{max} = 254$ nm) or by irradiation of methyl nitrite (CH_3ONO)/NO mixtures using 16−32 fluorescent lamps (Philips Tl 40W/05, $320 < \lambda < 450$ nm). Concentration−time profiles of reactants and products were recorded by long-path in situ FTIR spectroscopy. The FTIR spectrometer (Bruker IFS-88) was operated using a resolution of 1 cm^{-1} and a path length of 484.7 m. Most experiments were carried out at 1000 ± 20 mbar total pressure in synthetic air at 298 ± 2 K. However, in order to obtain mechanistic information some experiments were also performed in 1000 ± 20 mbar of N_2. During the irradiations 10 infrared spectra (128 interferograms co-added over ca. 2 min) were collected. Typical initial concentrations employed for the product studies were 0.7−1.0 ppm DNBM, 2−4 ppm CH_3ONO, 10−20 ppm H_2O_2, and 0.5−7 ppm NO (1 ppm = 2.46×10^{13} cm^{-3} at 1000 mbar and 298 K).

Since the infrared spectra of DNBM and its oxidation products, *n*-butoxymethyl formate (NBMF) and di-*n*-butyl carbonate (DNBC), are not available in the literature, calibrated IR spectra for these compounds have been measured and integrated band intensities (IBI) determined for the main absorption bands.

The IBIs for DNBM, NBMF, and DNBC were measured in the 1080 l quartz-glass room temperature photoreactor. In order to allow reproducible and quantitative transfer of the compounds into the gas phase, weighed amounts of the compound were dissolved in HPLC grade CH_3Cl and known volumes of the solution were subsequently injected into the reactor. The use of a solution in contrast to the pure compounds minimized interference by wall loss processes due to the low vapor pressure of this compound. The measurements were performed in 1000 mbar of N_2 at 298 K with spectrometer conditions as given above.

2.2. Outdoor Smog Chamber EUPHORE. Additional experiments on the OH-initiated oxidation of DNBM were carried out in the outdoor simulation chamber EUPHORE in Valencia, Spain. The chamber consists of a half-spherical 200 m^3 Teflon bag with a transmission of more than 80% in the range 280−640 nm. Two high-capacity ventilators ensure homogeneous mixing in the chamber. Cooling of the chamber floor compensates for the heating of the chamber by solar radiation. The photooxidation was initiated in the chamber by sunlight irradiation of a mixture of DNBM, nitrous acid (HONO) and NO_x in 1000 mbar of dry air. Concentration−time profiles of selected reactants and products were recorded using in situ FTIR-spectroscopy with a Nicolet Magna 550 spectrometer using a resolution of 1 cm^{-1} and a path length of 553.5 m. Each spectrum consisted of 550 interferograms co-added over a time period of 10 min. Typical initial concentrations were 350 ppb DNBM, 60 ppb HONO, 100 ppb NO, and 70 ppb NO_2. The mixtures were irradiated for approximately 3 h.

2.3. Relative Rate Technique. The rate coefficients for the reaction of OH with *n*-butoxymethyl formate (NBMF) and di-*n*-butyl carbonate (DNBC) were determined in the 1080 L photoreactor using the relative rate technique.[13] Since this method has already been described numerous times in the literature, it is only briefly outlined here. Provided that the reactant and the reference compound are removed solely by the reaction of interest and are not reformed in any process, which was the case for NBMF

$$\mathrm{OH} + \text{reactant} \rightarrow \text{products} \qquad \text{(R1)}$$

$$\mathrm{OH} + \text{reference} \rightarrow \text{products} \qquad \text{(R2)}$$

it can be shown that

$$\ln\frac{[\text{reactant}]_{t=0}}{[\text{reactant}]_t} = \frac{k_1}{k_2}\ln\frac{[\text{reactant}]_{t=0}}{[\text{reactant}]_t} \qquad (1)$$

where $[\text{reactant}]_{t=0}$ and $[\text{reactant}]_t$, and $[\text{reference}]_{t=0}$ and $[\text{reference}]_t$ are the reactant and reference concentrations at times $t = 0$ and t, respectively, and k_1 and k_2 are the rate coefficients for reactions R1 and R2.

A plot of $\ln([\text{reactant}]_{t=0}/[\text{reactant}]_t)$ versus $\ln([\text{reference}]_{t=0}/[\text{reference}]_t)$ yields a slope of k_1/k_2 with zero intercept. When there is an additional wall loss process for the reactant, which was the case for DNBC

$$\text{reactant} \xrightarrow{\text{wall}} \text{products} \qquad \text{(R3)}$$

the data can be analyzed using the following expression

$$\ln\frac{[\text{reactant}]_{t=0}}{[\text{reactant}]_t} - k_3 t = \frac{k_1}{k_2}\ln\frac{[\text{reactant}]_{t=0}}{[\text{reactant}]_t} \qquad (2)$$

where k_3 is the rate coefficient for reaction R3.

The kinetic experiments were performed in 1000 mbar air at 298 K using the photolysis of H_2O_2 as the OH radical precursor and 2-propanol ($k_{OH+isopropanol} = 5.7 \times 10^{-12}$ cm^3 $molecule^{-1}$ s^{-1})[14] and *n*-butane ($k_{OH+n-butane} = 2.17 \times 10^{-12}$ cm^3 $molecule^{-1}$ s^{-1})[14] as reference compounds. Typical initial concentrations for the kinetic experiments were 0.3−0.4 ppm DNBC, 0.3−0.4 ppm NBMF, 4 ppm *n*-butane, 1.0−1.5 ppm 2-propanol, and 25 ppm H_2O_2.

2.4. Chemicals and Gases. Di-*n*-butoxymethane (DNBM) (Lambiotte & Cie S.A, >99%), di-*n*-butyl carbonate (DNBC) (Lancaster, >98%), 2-propanol (Aldrich, >99.5%), and H_2O_2 (Peroxid Chemie, 85%) were used without further purification. All gases were supplied by Messer Griesheim and had the following stated purities: synthetic air (99.995%), N_2 (99.999%), NO (99.8%), NO_2 (98%), and *n*-butane (99.5%). The experiments in the EUPHORE reactor were performed in dried and purified air.[12]

Methyl nitrite was synthesized as described in the literature[15] by adding sulfuric acid dropwise to an ice-cooled mixture of methanol and sodium nitrite and collection in a cold trap at −78 °C.

HONO was synthesized by dropwise addition of 15 mL of a 1% $NaNO_2$ solution to 30 mL sulfuric acid (30%) at about 20 °C. The HONO formed in this reaction was flushed in an air stream into the dark EUPHORE chamber.

n-Butoxymethyl formate (NBMF) was synthesized in analogy to the synthesis of methoxymethyl formate described by Pihlaja et al.[16] and Weeks et al.[17] Briefly, 2 mol of finely ground sodium formate was placed in a flask, heated to 30 °C, and mixed with 0.5 mol *n*-butoxymethyl chloride. Mixing was stopped when the temperature in the system started to decrease. The product was extracted with ether. After drying by manganese sulfate, the solution was distilled under reduced pressure yielding pure NBMF. The purity of NBMF was determined by GC and NMR to be >98%.

2.5. Computer Simulation System. All computer simulations were carried out using the box model SBOX by Seefeld and Stockwell.[18,19] This FORTRAN program incorporating the Gear algorithm[20] was operated on an SGI Origin 200 workstation running under IRIX 6.5. The program uses the public domain library VODE[21] to integrate the ordinary differential equations.

3. Results and Discussion

3.1. Rate Coefficients for the Reaction of *n*-Butoxymethyl Formate (NBMF) and Di-*n*-butyl Carbonate (DNBC) with OH Radicals. Over the time period of all the experiments on NBMF, both adsorption on the wall and photolysis were negligible, whereas for DNBC an additional loss reaction due to wall adsorption was observed. This loss was well characterized by $k_{loss} = 1.5 \times 10^4\ s^{-1}$. Figure 1 shows examples of the data from the kinetic experiments plotted according to eq 1 and eq 2 for the reaction of OH with NBMF and DNBC, respectively. The rate coefficient ratios obtained from the slopes of such plots are given in Table 1 for the experiments on NBMF and DNBC with the two reference compounds 2-propanol and *n*-butane. Also given are the rate coefficients the reaction of OH with NBMF and DNBC derived from these ratios using the literature values for the analogue reactions with 2-propanol and *n*-butane. We choose to quote values for the rate coefficients, which are an average of all the experiments; hence

$$k_{OH + NBMF} = (8.00 \pm 0.91) \times 10^{-12}\ cm^3\ s^{-1}$$

$$k_{OH + DNBC} = (7.07 \pm 1.64) \times 10^{-12}\ cm^3\ s^{-1}$$

The quoted errors reflect the systematic errors due to the uncertainties in the rate coefficients of the reference compounds. They were derived from the standard deviations from averaging the values determined using the different reference compounds. Both the measured rate coefficients are about a factor of 4 lower than that for the reaction of OH with their atmospheric precursor DNBM. Taking an average OH concentration of $5 \times 10^6\ cm^{-3}$, typical for a summer day in a polluted region, the tropospheric lifetimes for NBMF and DNBC with respect to reaction with OH are 7.9 and 6.9 h, respectively. These fairly short lifetimes indicate that NBMF and DNBC will mainly be removed from the troposphere by reaction with OH. Transport to remote areas will be of minor importance. However, both compounds are highly water-soluble. Therefore, it can be assumed that, under appropriate conditions, wet deposition might also be an important tropospheric sink for these compounds.

3.2. Infrared Integrated Band Intensities (IBI) of Di-*n*-butoxymethane (DNBM), *n*-Butoxymethyl Formate (NBMF), and Di-*n*-butyl Carbonate (DNBC). Figure 2 shows infrared spectra which include that of DNBM (panel A) and NBMF (panel C) recorded with a resolution of 1 cm^{-1} in the region from 700 to 2000 cm^{-1}. The spectrum of DNBM contains a main absorption in the region of the C−O stretching vibration between 1000 and 1200 cm^{-1}. The spectrum of NBMF contains two main absorption bands, one in the region of the C═O stretching vibration between 1700 and 1790 cm^{-1} and one in the region of the C−O stretching vibration between 1000 and 1200 cm^{-1}. For the main bands of the DNBM and NBMF spectra and the two bands of the DNBC spectrum (not shown in Figure 2) the following integrated band intensities (IBI) have been calculated between the stated limits (the errors reflect the

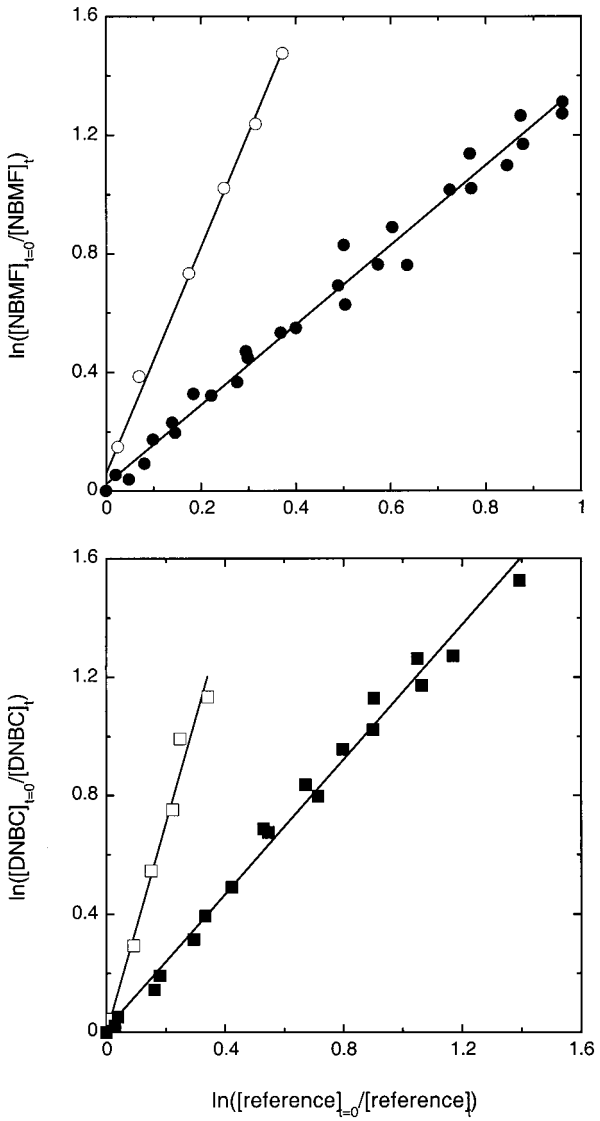

Figure 1. Plots of the kinetic data for the reaction of OH with *n*-butoxymethyl formate (NBMF) versus *n*-butane (○) and 2-propanol (●) (top) and di-*n*-butyl carbonate (DNBC) versus *n*-butane (□) and 2-propanol (■) (bottom). The solid lines are the results of linear least-squares fits to the corresponding data.

TABLE 1: Kinetic Data Obtained from the Investigations on the Reactions of OH with *n*-Butoxymethyl Formate (NBMF) and Di-*n*-butyl Carbonate (DNBC) at 298 ± 2 K

reactant	reference	$k_{reactant}/k_{reference}$	$k_{reactant} \times 10^{12}$ cm^3 molecule^{-1} s^{-1}
NBMF	isopropanol	1.35 ± 0.06	7.68 ± 0.34
	butane	3.84 ± 0.49	8.32 ± 0.49
DNBC	isopropanol	1.14 ± 0.05	6.49 ± 0.30
	butane	3.53 ± 0.42	7.65 ± 0.93

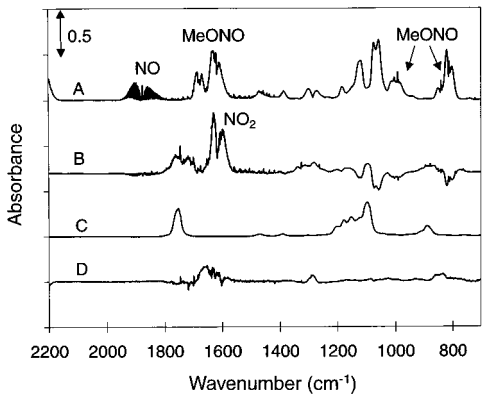

Figure 2. Infrared spectra recorded for a MeONO/NO_x/DNBM/air photolysis system in the wavenumber region 2000−700 cm^{-1}. Spectrum A was recorded before irradiation, B is a difference spectrum derived from a spectrum recorded after 10 min of irradiation minus spectrum A, C is a reference spectrum of *n*-butoxymethyl formate (NBMF), and D is the residual spectrum obtained after 10 min irradiation and subtraction of DNBM and all identified products multiplied by a factor of 5.

statistical 2σ precision only):

$$\text{DNBM:}\quad \text{IBI}\ (1100-1170\ \text{cm}^{-1}) = (1.35 \pm 0.04) \times 10^{-17}\ \text{cm molecule}^{-1}$$

$$\text{NBMF:}\quad \text{IBI}\ (1711-1786\ \text{cm}^{-1}) = (1.49 \pm 0.24) \times 10^{-17}\ \text{cm molecule}^{-1}$$

$$\text{IBI}\ (1060-1168\ \text{cm}^{-1}) = (2.10 \pm 0.23) \times 10^{-17}\ \text{cm molecule}^{-1}$$

$$\text{DNBC:}\quad \text{IBI}\ (1200-1354\ \text{cm}^{-1}) = (4.35 \pm 0.47) \times 10^{-17}\ \text{cm molecule}^{-1}$$

$$\text{IBI}\ (11725-1800\ \text{cm}^{-1}) = (1.24 \pm 0.16) \times 10^{-17}\ \text{cm molecule}^{-1}$$

3.3. Products of the OH-Initiated Oxidation of Di-*n*-butoxymethane (DNBM) in the Presence of NO_x. Figure 2 gives an example of the spectral information obtained from an experiment on a CH_3ONO/NO_x/DNBM system carried out in the indoor photoreactor. Spectrum A was recorded before irradiation. Spectrum B was obtained by subtraction of spectrum A from a spectrum recorded 10 min after irradiation. Spectrum C is a reference spectrum of *n*-butoxymethyl formate. Spectrum D is the residual product spectrum obtained after subtraction of all the identified compounds. This spectrum has been multiplied by a factor of 5 in order to highlight the residual absorptions.

In all systems investigated, *n*-butoxymethyl formate and propionaldeyhde were identified as the major products of the OH-initiated oxidation of DNBM in the presence of NO_x. In the indoor photoreactor runs using H_2O_2 as the OH radical precursor, formation of formaldehyde in high yield was observed. Di-*n*-butyl carbonate was identified as a minor product in all of the reaction systems. Additionally, formation of *n*-butyl formate and *n*-butoxymethyl butyrate in low yield was observed in the indoor photoreactor runs. The molar yields for the products in the different experimental systems have been obtained from the slopes of plots of the product concentration versus the amount of DNBM consumed. Examples of such plots for an experiment carried out in the indoor photoreactor are shown in Figure 3. The molar yields of all the products identified in the different experimental systems are summarized in Table 2. An upper limit of ≤10% for the yield of DNBC was estimated from the experimental data. For the yields of NBF and NBMB, an upper limit of ≤3% has been obtained for each compound.

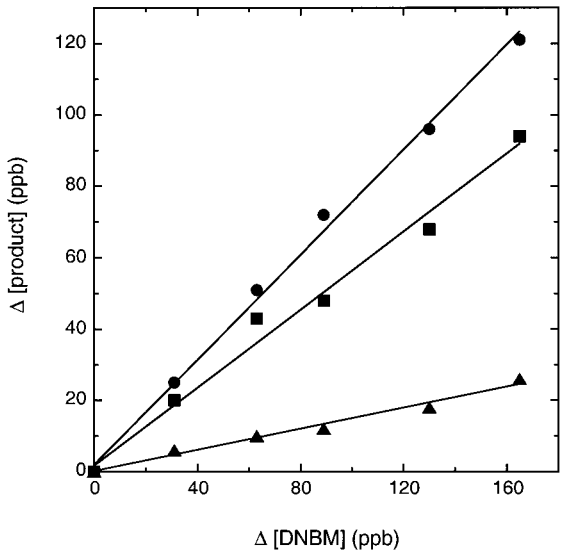

Figure 3. Formation of NBMF (●), propionaldehyde (■), and DNBC (▲) versus loss of DNBM for an example experiment. Initial conditions: 0.68 ppm DNBM, 15 ppm H_2O_2, and 6.0 ppm NO in air. The solid lines are the results of linear least-squares fits to the corresponding data.

TABLE 2: Molar Yields of the Major Products Obtained from Experiments on the OH-Radical-Initiated Oxidation of Di-*n*-butoxymethane (DNBM) in the Presence of NO_x[a]

	yield (mol %)		
experimental system	NBMF	propionaldehyde	HCHO
indoor photoreactor			
air/H_2O_2/NO_x/$h\nu$	88 ± 18	69 ± 14	25 ± 5
air/CH_3ONO/NO_x/$h\nu$	77 ± 15	78 ± 16	n. p.[b]
N_2/H_2O_2/NO_x/$h\nu$	76 ± 15	27 ± 5	50 ± 10
outdoor smog chamber			
air/HONO/$h\nu$	80 ± 8	44 ± 11	6 ± 3

[a] Minor products observed: di-*n*-butyl carbonate (DNBC, ≤10 mol %), *n*-butyl formate (NBF, ≤3 mol %), and *n*-butoxymethyl butyrate (NBMB, ≤3 mol %). [b] Determination not possible because of formaldehyde formation from CH_3ONO.

The yields of *n*-butoxymethyl formate, propionaldehyde, and formaldehyde were corrected for secondary reactions with OH radicals using an expression given by Atkinson et al.[22] This equation defines a correction factor F to be applied to the measured concentration in order to obtain the "true" concentration:

$$F = \frac{k_{\text{DNBM}} - k_{\text{product}}}{k_{\text{DNBM}}} \cdot \frac{1 - \dfrac{[\text{DNBM}]_t}{[\text{DNBM}]_{t=0}}}{\left(\dfrac{[\text{DNBM}]_t}{[\text{DNBM}]_{t=0}}\right)^{k_{\text{product}}/k_{\text{DNBM}}} - \dfrac{[\text{DNBM}]_t}{[\text{DNBM}]_{t=0}}} \quad (3)$$

where k_{DNBM} and k_{product} are the rate coefficients for the reactions of DNBM and the products (*n*-butoxymethyl formate, formaldehyde, or propionaldeyhde) with OH. $[\text{DNBM}]_{t=0}$ and $[\text{DNBM}]_t$ are the concentrations of DNBM at $t = 0$ and t,

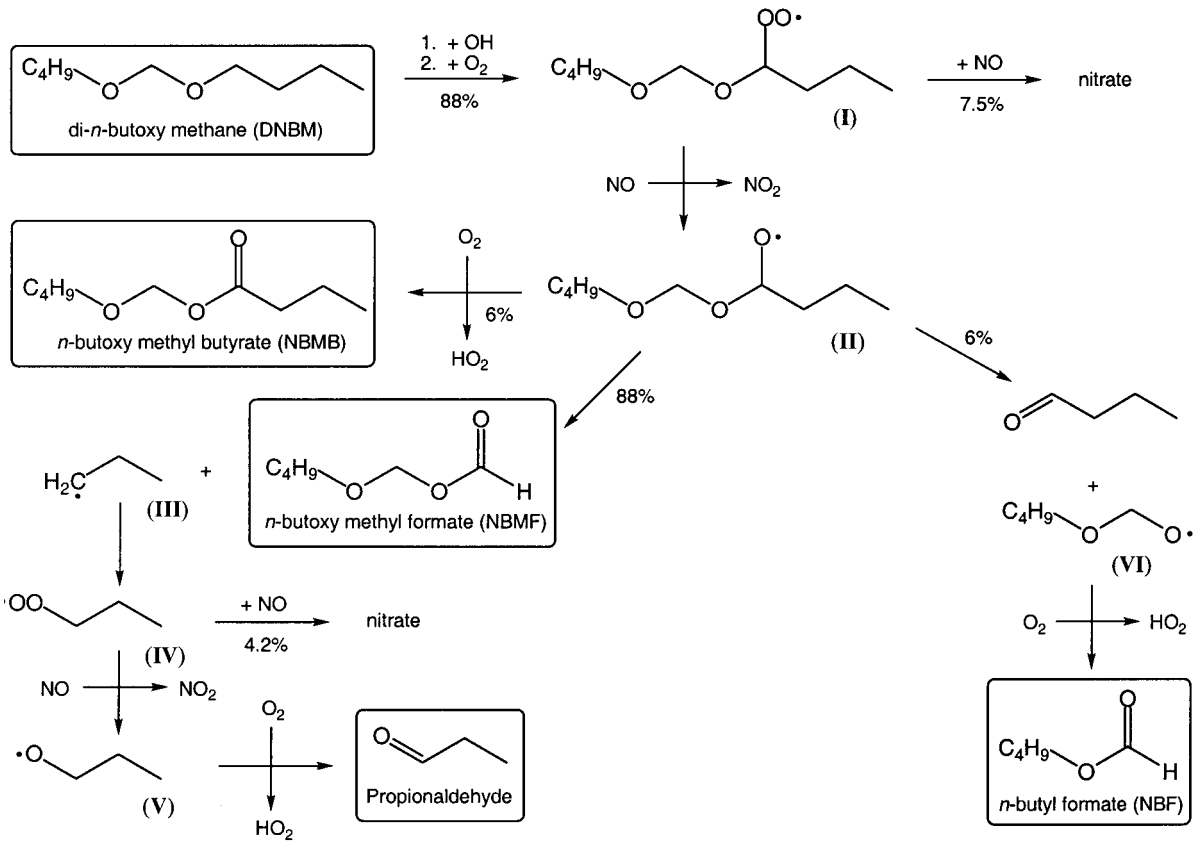

Figure 4. Tropospheric degradation scheme for the OH-initiated oxidation of DNBM in the presence of NO_x: OH attack at the α-CH_2 group of the butoxy group. The branching ratios given were determined by chemical modeling.

respectively. For the correction of the yields of *n*-butoxymethyl formate, propionaldeyhde, and formaldehyde, the following rate coefficients were used: $k_{OH+DNBM} = 3.21 \times 10^{-11}$ cm^3 s^{-1},[23] $k_{OH+NBMF} = 8.00 \times 10^{-12}$ cm^3 s^{-1}, $k_{OH+propionaldeyhde} = 1.96 \times 10^{-11}$ cm^3 s^{-1},[14] and $k_{OH+HCHO} = 9.6 \times 10^{-12}$ cm^3 s^{-1}.[14]

The reaction of OH with all other products is slow. Accordingly, its influence on the product yields obtained over the time scale of the experiments is negligibly small and the correction is not necessary.

In the residual product spectrum (see Figure 2, spectrum D), distinctive spectral features remain with bands at 1650, 1280, and 850 cm^{-1}. These absorptions are characteristic for organic nitrates, and lead to the conclusion that the OH-initiated oxidation of DNBM results in the formation of organic nitrates. Using the absorption cross section for octyl nitrate[24] of 1.25×10^{18} cm^3 molecule^{-1} at 1228 cm^{-1}, the overall yield for the sum of all nitrates formed in the OH-initiated oxidation of DNBM has been estimated to be ≤8−10%.

In all the systems investigated, *n*-butoxymethyl formate and propionaldehyde have been identified as the major products of the OH-initiated oxidation of DNBM in the presence of NO_x. In every experiment performed, the measured molar yield of *n*-butoxymethyl formate is, within the experimental errors, very similar. In the indoor photoreactor experiments, the yield of propionaldehyde measured in the absence of molecular oxygen is significantly lower than that observed in air. In contrast, the yield of formaldehyde in air is a factor of 2 lower than in the absence of O_2. This behavior can be rationalized from a consideration of the degradation mechanism for DNBM.

The OH-radical-initiated oxidation of DNBM proceeds via H atom abstraction. It is well-known that the preferred positions for OH attack on acetals of the general structure $ROCH_2OR$ are the $-CH_2-$ groups in α-position to the oxygen atoms.[25] For DNBM the OH radical attack will mainly occur at the $-CH_2-$ entities of the butyl side groups adjacent to the O atoms and also the central $-CH_2-$ group.

Figure 4 illustrates the reaction chain initiated by OH attack at the $-CH_2-$ entity of the butyl group, leading to the major products, *n*-butoxymethyl formate and propionaldehyde. H atom abstraction from the $-CH_2-$ entity forms the corresponding substituted alkyl radical. Addition of O_2 followed by reaction of the peroxy radical (**I**) with NO forms the alkoxy radical (**II**). Further reaction by cleavage of the C−C bond forms *n*-butoxymethyl formate and an *n*-propyl radical (**III**), which further reacts to form propionaldehyde. C−O bond cleavage forms butanal and an *n*-butoxymethoxy radical (**VI**). Reaction of radical **VI** with O_2 yields *n*-butyl formate. Because of the low upper limit of 3 mol % estimated for *n*-butyl formate and lack of experimental evidence for the formation of butanal, this reaction channel would appear to be of minor importance.

OH radical attack at the central $-CH_2-$ group of DNBM leads to di-*n*-butyl carbonate as illustrated in Figure 5. The initially formed substituted alkyl radical adds molecular oxygen yielding the peroxy radical (**VII**). Conversion of NO to NO_2 leads to the alkoxy radical (**VIII**), which further reacts with O_2 forming the stable carbonate.

As noted above, there is strong evidence for the formation of organic nitrates in the oxidation of DNBM. Accordingly, the reactions of the alkyl radicals **I**, **IV**, and **VII** (see Figures 4 and 5) with NO forming the corresponding nitrates seems to be reasonable. Isomerization reactions of the oxy radicals **II** and **VIII** appear to be negligible; this is supported by the nearly 100% carbon balance. The observation of only very weak absorptions in the residual product spectra also supports that isomerization products are probably not important.

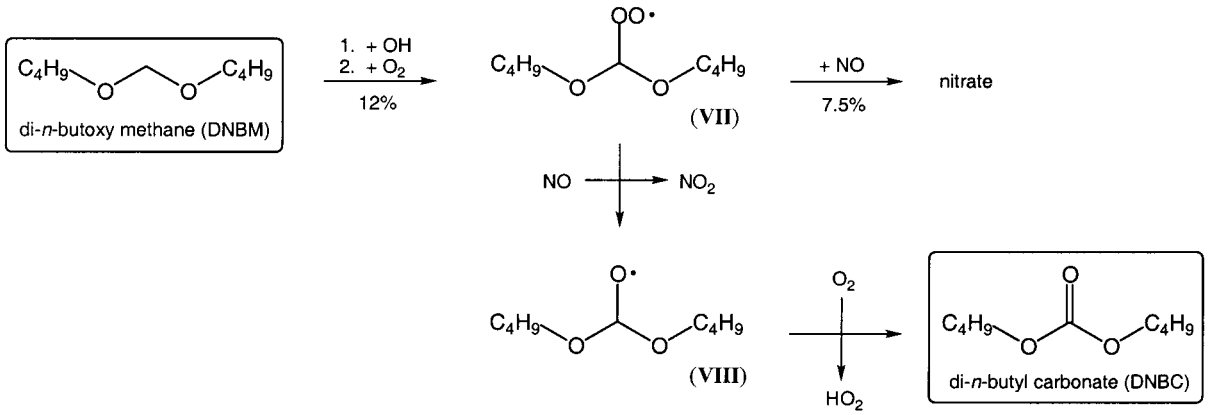

Figure 5. Tropospheric degradation scheme for the OH-initiated oxidation of DNBM in the presence of NO_x: OH attack at the central CH_2 group. The branching ratios given were determined by chemical modeling.

In order to ensure that the formation of *n*-butoxymethyl formate and propionaldehyde is initiated by H atom abstraction from the $-CH_2-$ entity of the butyl group adjacent to the O atom, experiments were performed in N_2. In N_2 the yield of propionaldehyde decreased significantly compared to air, whereas the yield of *n*-butoxymethyl formate remained constant and the yield of formaldehyde increased. This behavior is consistent with the degradation mechanism proposed in Figure 4. OH attack at the $-CH_2-$ entity of the butyl group adjacent to the O atom of DNBM is expected to lead to the formation of *n*-butoxymethyl formate and propionaldehyde in equivalent amounts when the oxygen partial pressure is sufficiently high. If the oxygen concentration is significantly reduced, the lifetime of radical **V** increases and C−C bond cleavage forming HCHO and an ethyl radical becomes possible and consequently the yield of propionaldehyde will decrease. In contrast, OH attack to the β-CH_2 position of the butoxy group of DNBM would directly form propionaldehyde by C−C bond scission. In this case the yield in propionaldehyde would be independent of oxygen partial pressure.

This observed behavior of the propionaldehyde yield in the experiments with and without O_2 thus confirms that *n*-butoxymethyl formate and propionaldehyde are formed via H atom abstraction from the $-CH_2-$ entity of the butyl group adjacent to the O atom.

The yield of propionaldehyde obtained in the outdoor smog chamber EUPHORE is significantly lower than in the indoor photoreactor. This is caused by removal of propionaldehyde from the system by photolysis. Under sunlight conditions, the rate of photolysis is notably higher than in the indoor photoreactor experiments, since the radiation intensity of the lamps used is much weaker. Accordingly, photolysis of propionaldehyde in the indoor chamber is negligible.

3.4. Chemical Modeling. An explicit reaction mechanism for the OH-initiated degradation of di-*n*-butoxymethane (DNBM) in the presence of NO_x was developed using a simple box model.[19] The reaction scheme was developed by fitting the model to the experimental concentration−time profiles for DNBM, the primary reaction products NBMF, propionaldehyde, DNBC, NO, NO_2, and methyl nitrite. The simulations were focused on the indoor photoreactor experiments using methyl nitrite photolysis as the precursor for OH radicals.

The reactions, describing the inorganic chemistry of the system, as well as the photolysis reactions, were taken from the RACM mechanism of Stockwell et al.,[26] which is widely used to model the chemistry occurring in urban air. The present mechanism was enhanced by the reactions describing the photolysis of CH_3ONO and the degradation of DNBM. The chemistry of CH_3ONO has been described in detail elsewhere.[27] The NO_2 photolysis rate ($J_{NO_2} = 3.76 \times 10^{-3}$ s^{-1} for 32 fluorescent lamps) was taken from previous measurements in the photoreactor.[28] The CH_3ONO photolysis rate cannot be obtained directly from the observed CH_3ONO decay since this compound is re-formed by recombination of CH_3O radicals with NO. However, photolysis of CH_3ONO is the most predominant OH source in the experiments and it was possible to obtain a value of $J_{CH_3ONO} = 8 \times 10^{-4}$ s^{-1} from a fit of the simulated VOC profiles to the experimental data. All other photolysis frequencies were evaluated relative to J_{NO_2} using the algorithm of Madronich.[29]

The degradation scheme developed for DNBM is listed in Table 3 and illustrated in the Figures 4 and 5. The rate coefficient for the reaction of OH radicals with *n*-butoxymethyl butyrate (NBMB) has not been measured and was estimated. NBMB has a molecular structure similar to that of *n*-butoxymethyl formate (NBMF). It seems reasonable to assume that both compounds will react with OH radicals with very similar rate coefficients. Accordingly, for the reaction OH + NBMB, a value of $k = 8.0 \times 10^{-12}$ cm^{3}s^{-1} was used in the present model.

In the modeling exercise the branching ratio of the initial reaction of OH with DNBM k_{R4}/k_{R16} and the nitrate from the reactions of peroxy radicals (**I** and **VII**) (R7 and R19) with NO were varied to provide the best fit of the experimental data. The product profiles were sensitive to the choice of k_{R4}/k_{R16} and the NO and NO_2 profiles were sensitive to the nitrate yield. Nitrate yields in reactions of peroxy radicals with NO are generally determined by the size of the peroxy radical. It was found that the best fits were achieved using k_{R4}:k_{R16} = 88:12 and a nitrate formation yield of 7.5% for reaction of NO with each of the peroxy radicals **I** and **VII** (R7 and R19). The total nitrate yield in the simulations is about 9.6 mol %, which agrees well with the upper limit of 8−10 mol % estimated from the experiments.

For DNBM the major fraction of the OH radical attack occurs at the $-CH_2-$ entity of the butyl group adjacent to the O atom (R4). Addition of O_2 to the alkyl radical formed and further conversion of NO to NO_2 by the corresponding peroxy radical leads to the oxy radical (**II**). The branching ratio for the reactions of **II** (R8−R10) was adjusted by fitting the model to the experimental data. The major reaction channel is the thermal decay forming NBMF and an *n*-propyl radical (R8). Further

TABLE 3: Chemical Mechanism for the OH-Initiated Oxidation of Di-*n*-butoxymethane (DNBM) in the Presence of NO_x Used for the Computer Simulations in the Present Work

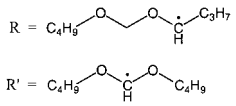

no.	reaction			k(298 K)[a]	ref
OH attack to DNBM in position 4					
R4	OH + DNBM	→	R + H_2O	2.83×10^{-11}	23[b]
R5	R + O_2 (+ M)	→	RO_2 (+ M)	1×10^{-11}	*c*
R6	RO_2 + NO	→	RO + NO_2	1×10^{-11}	*c*
R7	RO_2 + NO (+ M)	→	$RONO_2$ (+ M)	7.5×10^{-13}	*d*
R8	RO (+ M)	→	NBMF + $CH_3CH_2CH_2$(•) (+ M)	6.7×10^{5}	*d*
R9	RO (+ M)	→	*n*-$C_4H_9OCH_2O$(•) + n−C_4H_{10} (+ M)	4.0×10^{4}	*d*
R10	RO + O_2	→	NBMB + HO_2	8×10^{-15}	*c*
R11	$CH_3CH_2CH_2$(•) + O_2 + (M)	→	*n*-$C_3H_7O_2$ (+ M)	8.0×10^{-12}	
R12	*n*-$C_3H_7O_2$ + NO	→	*n*-C_3H_7O + NO_2	4.8×10^{-12}	30
R13	*n*-$C_3H_7O_2$ + NO (+ M)	→	*n*-$C_3H_7ONO_2$ (+ M)	2.1×10^{-13}	30
R14	*n*-C_3H_7O + O_2	→	C_2H_5CHO + HO_2	8×10^{-15}	30
R15	*n*-$C_4H_9OCH_2O$(•) + O_2	→	NBF + HO_2	8×10^{-15}	*c*
OH attack to DNBM in position 6 (center)					
R16	OH + DNBM	→	R′ + H_2O	3.85×10^{-12}	23[b]
R17	R′ + O_2 (+ M)	→	R′O_2 (+ M)	1×10^{-11}	*c*
R18	R′O_2 + NO	→	R′O + NO_2	1×10^{-11}	*c*
R19	R′O_2 + NO (+ M)	→	R′ONO_2 (+ M)	2.5×10^{-13}	*d*
R20	R′O + O_2	→	DNBC + HO_2	8×10^{-15}	*c*
reactions of primary products					
R21	OH + NBMF	→	products	8×10^{-12}	*e*
R22	OH + DNBC	→	products	7.1×10^{-12}	*e*
R23	OH + NBMB		products	8×10^{-12}	*f*
R24	OH + NBF	→	products	3.54×10^{-12}	
R25	OH + C_2H_5CHO	→	products	2×10^{-11}	
R26	C_2H_5CHO + $h\nu$	→	CH_3O + CO + HO_2	1.5×10^{-06}	26

[a] In cm^3 s^{-1} (second order) and s^{-1} (first order). [b] Derived from total rate coefficient,[23] ratio adjusted in this work to fit the chamber data. [c] Estimated from similar reactions.[14,30] [d] This work (estimated). [e] This work (measured). [f] Estimated from reaction R21.

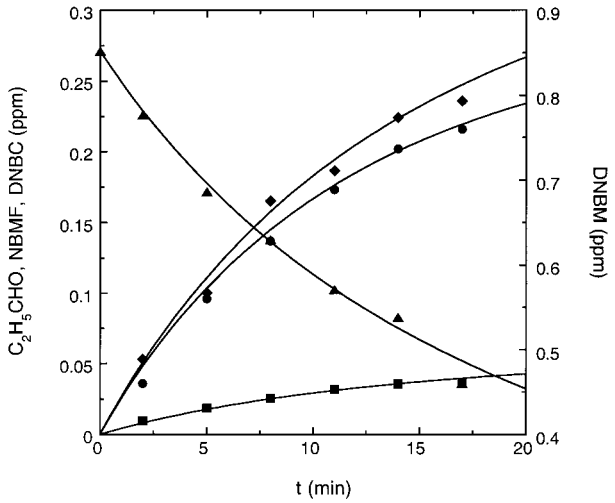

Figure 6. Oxidation of DNBM: comparison of experimental and simulated concentration−time profiles for DNBM (▲), NBMF (◆), propionaldehyde (●), and DNBC (■). The solid lines are the results of computer simulations. Initial conditions: 0.85 ppm DNBM, 6.0 ppm NO, 0.41 ppm NO_2, 1.28 ppm CH_3ONO, 760 Torr of air.

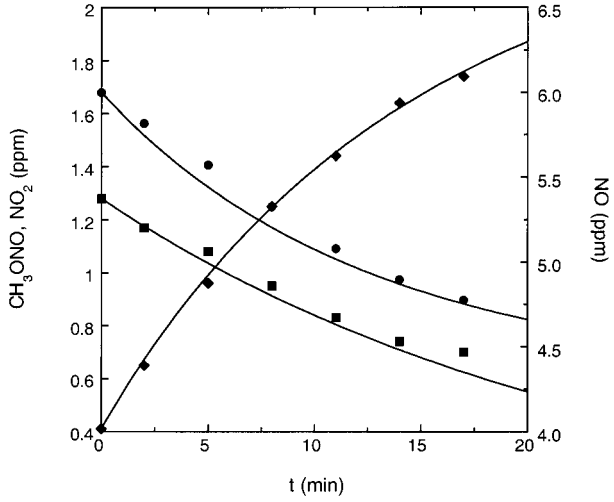

Figure 7. Oxidation of DNBM: comparison of experimental and simulated concentration−time profiles for methyl nitrite (■), NO (◆), and NO_2 (●). The solid lines are the results of computer simulations. For the initial conditions see Figure 6.

reaction of this *n*-propyl radical yields propionaldehyde, the second major product of the DNBM oxidation. Since upper limits for the formation of *n*-butyl formate and *n*-butoxymethyl butyrate (NBMB) were determined in the Experimental Section (see above), their formation reactions (R9 and R10) from radical **II** were also considered in the simulations. A small but nevertheless significant fraction of the OH radical attack occurs at the $-OCH_2O-$ group of DNBM (R16) which leads to formation of di-*n*-butyl carbonate (DNBC) and small amounts of the corresponding nitrate (see Figure 5).

In total, the chemical model used in the present work consisted of 76 elementary reactions. Figures 6 and 7 demonstrate the quality of the fits achieved. For all the reactants illustrated, experimental and modeled concentration−time profiles are in excellent agreement.

4. Summary and Conclusions

The atmospheric oxidation of di-*n*-butoxymethane (DNBM) was studied in the presence of NO_x. The major reaction products in air are *n*-butoxymethyl formate (NBMF) and propionaldeyhde with a molar yield of ~80 mol % for each compound. Further products formed in smaller amounts are di-*n*-butyl carbonate (DNBC), *n*-butyl formate (NBF) and *n*-butoxymethyl butyrate (NBMB).

For the reactions of OH radicals with NBMF and DNBC, bimolecular rate coefficients of $k_{OH+NBMF} = (8.00 \pm 0.91) \times 10^{-12}$ cm^3 s^{-1} and $k_{OH+DNBC} = (7.07 \pm 1.64) \times 10^{-12}$ cm^3 s^{-1}, respectively, were determined for the first time. From these data, tropospheric lifetimes of several hours for each of both compounds were calculated. These relatively short lifetimes indicate that reaction with OH will be the dominant sink for both NBMF and DNBC and that transport to remote areas will play a minor role in their regional and global atmospheric chemistry. Due to their water solubility, wet deposition of these compounds will probably also be an additional removal path.

For the OH-initiated degradation of DNBM in the presence of NO_x, a chemical mechanism has been constructed. Experimental and modeling results are in excellent agreement. After further validation tests under realistic atmospheric conditions in the presence of other VOCs, the developed reaction scheme will be able to be used in applications such as field modeling.

Acknowledgment. Financial support of the work by the European Commission and the Bundesministerium für Bildung und Forschung (BMBF) is gratefully acknowledged.The sample of di-*n*-butoxymethane was supplied by Lambiotte & Cie S.A., Brussels. The authors thank W. R. Stockwell, Reno, NV, for the supply of software and very helpful discussions. L.T. acknowledges the cooperation of the CEAM employees at EUPHORE and financial support by the Generalidad Valenciana, Fundación BANCAIXA and the Deutscher Akademischer Austauschdienst (DAAD).

References and Notes

(1) Hälsig, C. P.; Gregory, R.; Peacock, T. *Spec. Publ.—R. Soc. Chem. Chem. Oil Ind.: Dev. Appl.* **1991**, *97*, 311.

(2) Dolislager, L. J. *J. Air Waste Manage. Assoc.* **1997**, *47*, 775.

(3) Guttmann H.; Schug, K. P. SAE Technical Paper Series, No. 900274, Society of Automotive Engineers, Warrendale, PA, 1990.

(4) CONCAWE Automotive Emissions Management Group, Report No. 2/95, Brussels, Belgium, 1995.

(5) Dodge, L.; Naegeli, D. W. Final Report No. NREL/-TP-425-6345, National Renewable Energy Laboratory, Golden, CO, 1994.

(6) Wallington, T. J.; Hurley, M. D.; Ball, J. C.; Straccia, A. M.; Platz, J.; Christensen, L. K.; Sehested, J.; Nielsen, O. J.; *J. Phys. Chem. A* **1997**, *101*, 5302.

(7) Reuter, R. M.; Benson, J. D.; Burnes, V. R.; Gorse, R. A.; Hochhauser, A. M.; Koehl, W. J.; Painter, L. J.; Rippon, B. H.; Rutherford, J. A. SAE Technical Paper Series, No. 920326, Society of Automotive Engineers, Warrendale, PA, 1992.

(8) Squillace, P. J.; Zogorski, J. S.; Wilber , W. G.; Price, C. V. *Environ. Sci. Technol.* **1996**, *30*, 1721.

(9) Morse, P. M. *Chem. Eng. News* **1999**, *77*, 26.

(10) Thüner, L. P. Barnes, I., Maurer, T. Sauer, C. G.; Becker, K. H. *Int. J. Chem. Kinet.* **1999**, *31*, 797.

(11) Barnes, I.; Becker, K. H.; Mihalopoulos, N. *J. Atmos. Chem.* **1994**, *18*, 267.

(12) Becker, K. H., Ed. The European Photoreactor EUPHORE, Final Report, EV5V-CT92-0059 1996.

(13) Bierbach, A.; Barnes, I.; Becker, K. H.; Wiesen, E. *Environ. Sci. Technol.* **1994**, *28*, 715.

(14) Atkinson, R. *J. Phys. Chem. Ref. Data* **1994**, Monograph No. 2.

(15) Taylor, W. D.; Allston, T. D.; Moscato, M. J.; Fazekas, G. B.; Kozlowski, R.; Takacs, G. A. *Int. J. Chem. Kinet.* **1980**, *12*, 231.

(16) Pihlaja, K.; Lampi, A. *Acta Chim. Scand. B* **1986**, *40*, 196.

(17) Weeks, D. P.; Field, F. H. *J. Am. Chem. Soc.* **1970**, *92*, 1600.

(18) Seefeld, S. Ph.D. Thesis, Swiss Federal Institute of Technology Zurich (ETH), Switzerland, 1997.

(19) Seefeld, S.; Stockwell, W. R. *Atmos. Environ.* **1999**, *33*, 2941.

(20) Gear, C. W. *Prentice Hall Series in Automatic Computation*; Prentice-Hall: Englewood Cliffs, NJ, 1971; Vol. 17.

(21) Brown, P. N.; Byrne, G. D.; Hindmarsh, A. C. *J. Sci. Stat. Comput.* **1989**, *10*, 1038.

(22) Atkinson, R.; Aschmann, S. A.; Carter, W. P. L.; Winer, A. M.; Pitts, J. N., Jr. *J. Phys. Chem.* **1982**, *86*, 4563.

(23) Becker, K. H.; Dinis, C.; Geiger, H.; Wiesen, P. *Chem. Phys. Lett.* **1999**, *300*, 460.

(24) Wirtz, K. Ph.D. Thesis, University of Wuppertal, FRG, 1991.

(25) Becker, K. H.; Freitas Dinis, C. M.; Geiger, H.; Wiesen, P. *Phys. Chem. Chem. Phys.* **1999**, *1*, 4721, and references therein.

(26) Stockwell, W. R.; Kirchner, F.; Kuhn, M.; Seefeld, S. *J. Geophys. Res.* **1997**, *102*, 25847.

(27) Geiger, H.; Becker, K. H. *Atmos. Environ.* **1999**, 33, 2883.

(28) Sauer, C. G.; Barnes, I.; Becker, K. H.; Geiger, H.; Wallington, T. J.; Christensen, L. K.; Platz, J.; Nielsen, O. J. *J. Phys. Chem. A* **1999**, *103*, 5959.

(29) Madronich, S. *J. Geophys. Res*. **1987**, *92*, 9740.

(30) DeMore, W. B.; Sander, S.; Howard, C. J.; Ravishankara, A. R.; Golden, D. M.; Kolb, C. E.; Hanson, R. F.; Kurylo, M. J.; Molina, M. J. Chemical Kinetics and Photochemical Data for Use in Stratospheric Modeling, Evaluation No. 12, JPL Publication 97-4, Pasadena, CA, 1997.

(31) Le Calvé, S.; Le Bras, G.; Mellouki, A. *J. Phys. Chem. A* **1997**, *101*, 5489.

(32) Atkinson, R.; Baulch, D. L.; Cox, R. A.; Hampson, Jr., R. F.; Kerr, J. A.; Rossi, M. J.; Troe, J. *J. Phys. Chem. Ref. Data* **1997**, *26*, 521.